

# Improved Transmucosal Delivery of Glimepiride via Unidirectional Release Buccal Film Loaded With Vitamin E TPGS-Based Nanocarrier

Dose-Response:  
An International Journal  
July-September 2020:1-12  
© The Author(s) 2020  
Article reuse guidelines:  
sagepub.com/journals-permissions  
DOI: 10.1177/1559325820945164  
journals.sagepub.com/home/dos



Tahani S. Basahih<sup>1</sup>, Abdullah A. Alamoudi<sup>1</sup>, Khalid M. El-Say<sup>1</sup>,  
Nabil A. Alhakamy<sup>1,2</sup>, and Osama A. A. Ahmed<sup>1</sup> 

## Abstract

Glimepiride (GMD) is a hypoglycemic agent that has variation in bioavailability for its unexpected absorption. Glimepiride was formulated in a buccal film loaded with a nanobased formulation to enhance its absorption via buccal mucosa. Nanostructured lipid carriers (NLCs) and D- $\alpha$ -tocopherol polyethylene glycol 1000 succinate-based micelles enhance GMD solubility and improve its permeation through the buccal mucosa. The formulation variables were optimized using a Box-Behnken design. These factors, such as the percent of micelles relative to NLC ( $X_1$ ), the percent of Carbopol ( $X_2$ ), and the percent of permeation enhancer ( $X_3$ ), were investigated for their effect on the initial release ( $Y_1$ ) and the cumulative release after 6 hours ( $Y_2$ ). The optimum levels for  $X_1$ ,  $X_2$ , and  $X_3$  were 100%, 0.05%, and 1.8%, respectively. The optimized formulation revealed that the permeation of GMD from the film was in favor of micelles. This optimized film was then coated with ethyl cellulose to direct the release only through the buccal mucosa. The optimized unidirectional GMD transmucosal film showed a release of 93.9% of GMD content at 6 hours compared to 60.41% of GMD release from the raw GMD film. This finding confirmed the suitability of transmucosal delivery of GMD via the buccal mucosa.

## Keywords

glimepiride, transmucosal film, experimental design, micelles, nanostructured lipid carriers, D- $\alpha$ -tocopherol polyethylene glycol 1000 succinate

## Introduction

Diabetes is a multimetabolic disorder known by elevated blood sugar levels resulting from a deficiency in insulin release or insulin performance or both.<sup>1</sup> Glimepiride (GMD) is an efficient and well-endured hypoglycemic drug for the treatment of type 2 diabetes.<sup>2,3</sup> Glimepiride is a third-generation sulfonylureas (SUs) that developed attention because it shows a unique pharmacological and pharmacokinetic aspects, compared to the earlier first- and second-generation SUs. Glimepiride is a water-insoluble drug that demonstrates a decreased pH-dependent solubility.<sup>4</sup> In both acidic and neutral aqueous media, GMD shows very poor solubility at 37 °C (<0.004 mg/mL). In basic media pH > 7, the solubility of the GMD is a little elevated to 0.02 mg/mL. This inadequate solubility profile of GMD may originate a poor dissolution and unexpected bioavailability.<sup>5,6</sup>

The need to formulate GMD for improved delivery was originated from the designing problems of its pharmaceutical formulations. Glimepiride has a very poor aqueous solubility and

wettability that led to these problems and consequently changes in oral bioavailability.<sup>7</sup> Buccal drug delivery includes the introduction of active pharmaceutical ingredients via buccal mucosa (the coating of the oral cavity).<sup>8-10</sup> It protects the drug from the first-pass metabolism and degradation in the acidic environment as the drug is delivered via the buccal route.<sup>11</sup>

Nanostructured lipid carriers (NLCs), manufactured by physiological lipid materials with a solid form at room temperature,

<sup>1</sup> Department of Pharmaceutics, Faculty of Pharmacy, King Abdulaziz University, Jeddah, Saudi Arabia

<sup>2</sup> Center of Excellence for Drug Research and Pharmaceutical Industries, King Abdulaziz University, Jeddah, Saudi Arabia

Received 15 May 2020; received revised 19 June 2020; accepted 29 June 2020

## Corresponding Author:

Osama A. A. Ahmed, Department of Pharmaceutics, Faculty of Pharmacy, King Abdulaziz University, Jeddah 21589, Saudi Arabia.

Email: oaahmed@kau.edu.sa



offer advantages as a nanocarrier system such as biocompatibility, improved bioavailability, and biodegradability.<sup>12,13</sup> The other example of nanocarrier is micelles made with vitamin E prodrug D- $\alpha$ -tocopheryl polyethylene glycol 1000 succinate known as the TPGS micelle system, which paved the way for a new approach in delivering both kinds of drugs hydrophilic and hydrophobic either with or without imaging agents. The amphipathic properties of TPGS as a novel nonionic surfactant generate stable micelles in low concentration, by about 0.02 wt% in the aqueous medium. Numerous TPGS-based formulations have been introduced since the Food and Drug Administration approved TPGS as a safe pharmaceutical supplement.<sup>14</sup> Several advantages can be listed with the usage of TPGS in drug delivery for its biological and physicochemical properties. For example, TPGS has an elevated level of biocompatibility, promotes drug permeation, and enhances solubility.<sup>15</sup>

This study aimed to prepare GMD-nanocarrier (NLCs and/or micelles) loaded into a transmucosal buccal film to avoid variations in solubility profile, minimize gastric disturbance issues, and improve patient adherence to GMD and compliance. The prepared GMD films were characterized for thickness, stretching (elasticity), drug content, and optimized using experimental design for the initial and cumulative GMD release. Furthermore, the optimized GMD film was characterized for mucoadhesion, initial, and cumulative GMD release. The optimized GMD film was prepared as a unidirectional release buccal film and investigated for the ex vivo permeation and fluorescence laser microscope study.

## Materials

Glimepiride was a kind gift from Spimaco AddwaeiH, Al-Qassim, KSA. D- $\alpha$ -Tocopheryl polyethylene glycol 1000 succinate Bioextra (TPGS), hydrogenated phosphatidylcholine from soybean, almond oil, Carbopol 934 (CRP), ethanol, and chloroform were from Sigma-Aldrich. Hydroxypropyl methylcellulose (HPMC) 4000 cp was from Spectrum Chemical Manufacturing Corporation. All chemicals were of analytical grade.

## Methods

### Preparation of GMD-TPGS Micelles

The GMD micelles were prepared with vitamin E TPGS (TPGS) utilizing a previously reported method.<sup>16</sup> Briefly, TPGS was dissolved in 15-mL ethanol while GMD was dissolved in 2 mL of warm chloroform until completely dissolved. The GMD solution was then poured into TPGS solution with stirring in a water bath at 50 °C (GFL) for 30 seconds, then 35 mL of distilled water was added. The organic solvent (ethanol and chloroform) was removed using rotavapor (BUCHI labortechnik AG). The final volume was adjusted to 50 mL by distilled water.

### Preparation of GMD-NLCs

Nanostructured lipid carriers were prepared by the hot emulsification-ultrasonication technique.<sup>17,18</sup> Briefly, GMD was mixed with the lipids, namely, almond oil, Compritol, and

**Table 1.** Box-Behnken Design Attributes Involving Factors and Their Selected Levels With Responses and Their Constraints and Goals.

| Factors  | Low   | High  | Units    |
|--|-------|-------|----------|
| X <sub>1</sub> : The percentage of micelles relative to NLCs         | 0     | 100   | %        |
| X <sub>2</sub> : The concentration of CRP in percent                 | 0.05  | 0.1   | %        |
| X <sub>3</sub> : The concentration of permeation enhancer in percent | 0     | 2     | %        |
| Response   | Low   | High  | Goal     |
| Y <sub>1</sub> : Initial release (%)                                 | 10.36 | 23.45 | Maximize |
| Y <sub>2</sub> : Cumulative release (%)                              | 83.27 | 98.91 | Maximize |

Abbreviations: CRP, Carbopol; NLCs, nanostructured lipid carriers.

phosphatidylcholine (phospholipid), in 30-mL chloroform at 80 °C. Then chloroform was removed using rotavapor (BUCHI labortechnik). Gelucire 44/14 was dissolved in 30-mL distilled water at 80 °C with stirring until complete dissolution takes place. The dissolved Gelucire solution was added to the lipid mixture containing GMD at 80 °C and then homogenized for 3 minutes (T 25 ULTRA-TURRAX), followed by ultrasonication using Sonics VC750 at 80 °C with 35% amplitude for 3 minutes to obtain an emulsion. Finally, distilled water was used to adjust the final volume to 50 mL and set aside to cool at 20 °C.

### Particle Size Characterization of GMD Nanocarriers

The particle size of the prepared nanoparticles was measured using Zetasizer Nano ZSP (Malvern Panalytical Ltd). A sample, from each nanoformulation, was diluted to 20-fold with distilled water before measurement that was carried out in triplicates and the average size was recorded.

### Formulation and Optimization of GMD-Loaded Buccal Film

Fifteen formulations were suggested by Box-Behnken design (BBD), using Statgraphics 18 Centurion Software, to optimize the release behavior of GMD from the buccal film. In this study, a 3-level 3-factor design with 2 responses was endorsed. The variables are the percentage of micelles relative to NLCs (X<sub>1</sub>), the concentration of CRP in percent (X<sub>2</sub>), and the concentration of permeation enhancer in percent (X<sub>3</sub>), while the response parameters are the percentage of initial release (Y<sub>1</sub>) and the percentage of cumulative release after 6 hours (Y<sub>2</sub>; Table 1). Hydroxypropyl methylcellulose was used as a film-forming polymer in 2% (wt/vol). Based on the BBD, randomized 15 formulations of the buccal film were produced as seen in Table 2. The prepared films are fully characterized and evaluated for release behavior. The obtained data are analyzed using analysis of variance followed with the multiple response optimization. The optimum concentrations for the 3 variables were established to develop GMD-loaded buccal film with an optimum drug-release profile.

**Table 2.** Experimental Matrix of GMD-Loaded Buccal Film as Suggested by Box-Behnken Design With the Observed and the Fitted Values of the Responses ( $Y_1$  and  $Y_2$ ).<sup>a</sup>

| Run # | $X_1$ (%) | $X_2$ (%) | $X_3$ (%) | Initial release (%) |              | Cumulative release (%) |              |
|-------|-----------|-----------|-----------|---------------------|--------------|------------------------|--------------|
|       |           |           |           | Observed value      | Fitted value | Observed value         | Fitted value |
| 1     | 100       | 0.075     | 2         | 21.78               | 21.64        | 98.43                  | 98.42        |
| 2     | 0         | 0.05      | 1         | 13.96               | 13.75        | 86.91                  | 86.83        |
| 3     | 100       | 0.1       | 1         | 18.99               | 19.20        | 97.11                  | 97.19        |
| 4     | 100       | 0.075     | 0         | 20.12               | 20.52        | 97.87                  | 97.77        |
| 5     | 50        | 0.075     | 1         | 15.99               | 16.25        | 91.58                  | 91.47        |
| 6     | 100       | 0.05      | 1         | 23.45               | 22.98        | 98.91                  | 98.93        |
| 7     | 50        | 0.075     | 1         | 16.46               | 16.25        | 91.21                  | 91.47        |
| 8     | 50        | 0.1       | 2         | 15.23               | 15.16        | 90.97                  | 90.89        |
| 9     | 50        | 0.05      | 0         | 17.42               | 17.49        | 92.01                  | 92.09        |
| 10    | 50        | 0.075     | 1         | 16.29               | 16.25        | 91.63                  | 91.47        |
| 11    | 0         | 0.1       | 1         | 10.36               | 10.83        | 83.27                  | 83.25        |
| 12    | 50        | 0.05      | 2         | 18.02               | 18.63        | 93.15                  | 93.14        |
| 13    | 0         | 0.075     | 2         | 13.12               | 12.73        | 86.12                  | 86.22        |
| 14    | 50        | 0.1       | 0         | 14.87               | 14.26        | 88.99                  | 89.01        |
| 15    | 0         | 0.075     | 0         | 11.67               | 11.81        | 83.92                  | 83.93        |

Abbreviations: GMD, glimepiride;  $X_1$ , the percentage of micelles relative to NLCs;  $X_2$ , the concentration of CRP in percent;  $X_3$ , the concentration of permeation enhancer in percent;  $Y_1$ , initial release (%);  $Y_2$ , cumulative release (%).

<sup>a</sup>The observed values of  $Y_1$  and  $Y_2$  represent the means of 3 determinations; standard deviations were <5% of the mean and thus are omitted from the table.

### Preparation of GMD-Loaded Buccal Film

Buccal films were prepared by the solvent casting method. The prepared nanocarrier dispersions were mixed with HPMC as a film-forming polymer, Carbopol as a mucoadhesive polymer, and sodium cholate hydrate as a permeation enhancer with constant stirring for 15 minutes using a mechanical stirrer. Propylene glycol (2% [wt/vol]) was used as a plasticizer. The solution was then homogenized (IKA T18 basic homogenizer, IKA, Works da Brasil Lida Taquara) at 18 000 rpm for 3 minutes, stored in the refrigerator for 48 hours, then sonicated (QS3 ultrasonic cleaner, the United Kingdom) for 5 minutes to remove any residual air bubbles. This solution was then poured into a Petri dish of 9 cm in diameter, covered with pierced aluminum foil and dried in a vacuum oven at 40 °C until completely dried, and finally placed in a desiccator for 24-hour before being stored in the freezer for the following characterization step.

### Characterization of the Prepared Buccal Films

#### Thickness Measurement

The thickness of the film was measured using Digimatic Micrometer (Kawasaki). For each formulation, 3 different points were selected randomly and measured. An average was then calculated.

#### Stretching Evaluation

A part of the film of area 4 cm × 1 cm was picked randomly and tested for its stretching tension. The stretching of the film was evaluated as described previously using a modified

elongation testing apparatus that was designed in our laboratory.<sup>19,20</sup> Briefly, the film was placed between 2 clamp jaws, separated by 2 cm, the lower one was attached by a constant weight of 200 g, this film was held for 1 minute, and the change of its length was recorded if there is any, and the elongation percent was calculated according to the following equation:

$$\text{Elongation (\%)} = \left( \frac{L_f - L_0}{L_0} \right) \times 100, \quad \text{Equation (1)}$$

where  $L_f$  is the length of the film at the end of the experiment and  $L_0$  is the original patch length.

#### Drug Content

A one square centimeter portion was chosen randomly from the film to determine its drug content. Each portion was placed into 20 mL of chloroform in a closed vial in a warm shaking water bath (GFL) of 37 °C, left overnight until complete solubilization takes place, then a sample was taken for high-performance liquid chromatography (HPLC) analysis. This procedure was repeated 3 times and an average was recorded.

#### Ex Vivo Permeation of GMD Buccal Films

The release of GMD from the prepared films and its permeation through buccal mucosa was carried out using a modified USP dissolution test apparatus (Pharma test).<sup>21,22</sup> A buccal mucosa, freshly isolated from goat and collected from the slaughterhouse, was soaked for 2 hours in a phosphate buffer (pH 7). The isolated mucosa was then stretched around one end of a double-end open glass tube, making the effective surface area of the membrane equal to 3.14 cm<sup>2</sup> diameter. The whole tube (donor compartment) was hung on a rolling paddle (receptor

compartment) with the mucosa in contact with the receptor medium. Glimpiride buccal films (1 cm<sup>2</sup> area of each formula) were introduced into the donor tube. The vessel contains 500-mL phosphate buffer solution pH 7, at 37 °C ± 0.5 °C and stirred at 50 rpm.<sup>21</sup> Aliquots of 3-mL samples were withdrawn from the receptor medium at time points intervals and replaced with equal volumes of fresh buffer.

### High-Performance Liquid Chromatography Analysis of GMD

The drug content and GMD released was analyzed using Agilent 1200 series HPLC system (Agilent) for the determination of GMD content and the percent permeated across the buccal mucosa. Using the methods of El-Enany et al and Ahmed et al with some modifications,<sup>23,24</sup> a C18 (250 mm, 4.6 mm ID, 5-µm particle size) column from Cole-Parmer (Vernon Hills) was used, acetonitrile: 0.02 M phosphate buffer pH 5 (60/40, vol/vol) as the mobile phase, the flow rate was 1.5 mL/min and 238 nm UV detection. The results obtained were the average of 3 measurements.

### Prediction of the Optimized GMD Buccal Film

Based on the data obtained from the responses ( $Y_1$  and  $Y_2$ ), the optimized formula was determined by considering all the significant factors that affect each response. This was achieved by analyzing the obtained experimental results using the Statistics software.

### Characterization of the Prepared Optimized GMD Buccal Film

The proposed optimized GMD-film formulation was characterized for the parameters as the 15 runs that have been previously performed (thickness, stretching, size, and drug content). The data obtained for the initial and the cumulative drug release were compared with the predicted values.

### Mucoadhesion Test for the Optimized GMD Film

Mucoadhesion test of the optimized GMD film was carried out ex vivo by applying to fresh-cut sheep buccal mucosa (1 cm<sup>2</sup> area). The tissue was immersed in phosphate buffer solution (pH 4.5) at 37 °C for equilibration before carrying out the mucoadhesive test. The tissue was fixed using glue on a flat plate fitted to the lower grip of the Tensile Tester Machine (Shimadzu Co).<sup>25</sup> The optimized GMD film (1 cm<sup>2</sup> area) was fixed to the upper blade of the Tensile Tester and kept contacting the mucosa for 2 minutes. After that, the detachment force (tensile strength) was recorded. The experiment was carried out in triplicate.<sup>26,27</sup> Mucoadhesive strength was then calculated by equation 2.

$$\text{Tensile strength (N/mm}^{-2}\text{)} = \frac{\text{Force of break (N)}}{\text{Area of the sample(mm}^2\text{)}} \quad \text{Equation (2)}$$

### Preparation of Unidirectional-Release GMD Films

The optimized GMD film was cut into circles with a surface area of 1.54 cm<sup>2</sup>. The cut circles were sprayed with 0.5 mL ethylcellulose solution (2%, wt/vol in acetone) onto the surface of the film using an oral spray bottle (RPC Plastiap) and immediately oven-dried at 70 °C for 5 minutes. This procedure was repeated until an ethylcellulose layer was formed on the surface of the optimized GMD film.<sup>28</sup>

### Optimized GMD Bilayer Unidirectional Buccal Film Ex Vivo Permeation Study

The diffusion of GMD from the prepared buccal films, either contain pure (raw) drug or optimized formula, was carried out utilizing the same conditions for the method previously mentioned in the ex vivo permeation of GMD buccal films.

### Fluorescence Laser Microscope Study of Optimized GMD Bilayer Unidirectional Buccal Film

The transport of GMD-optimized formula through buccal mucosa layers was studied using Zeiss Axio Observer D1 inverted DIC Fluorescence microscope (Carl Zeiss AG). Nanovesicles loaded with fluorescence isothiocyanate (FITC), instead of GMD, was prepared and loaded into the optimized buccal film as previously described. A pure FITC-loaded buccal film was also prepared as a control. Both films were applied to the excised buccal mucosa that was mounted on the Franz diffusion cell apparatus. The buccal mucosa was removed after 0.5 and 6 hours. The collected samples were kept in formalin. A longitudinal section in each sample using a microtome blade was done from paraffin wax buccal mucosa samples. Images were taken using 270/40 nm excitation, 495 nm beam splitter, and 525/50 nm emission.

## Results and Discussion

### Preparation and Characterization of GMD Nanovesicles

The prepared GMD-loaded micelles showed an average particle size of 14.00 ± 3.60 nm (Figure 1A). On the other hand, GMD-loaded NLCs showed a nanosize average of 137.77 ± 15.39 nm (Figure 1B). Nanodispersion drug carriers are utilized to improve pharmacological efficiency and reduce toxic side effects for the loaded drugs.<sup>29</sup> TPGS-based micelles have shown great promise for improving drug solubility and delivery.<sup>15,16,30,31</sup> The micelles were formed in the solution following the change of the solvent from organic to aqueous. The change of the solvent in the solution was done gradually, in order to avoid GMD precipitation. The solvent of choice was ethanol, due to its high-water miscibility and low vapor pressure, which simplified the solvent removal.

In addition, lipid-based drug carriers are promising delivery systems because of their potential to improve solubility and bioavailability of the loaded drugs either water soluble or poorly water soluble.<sup>32,33</sup> Nanostructured lipid carriers were

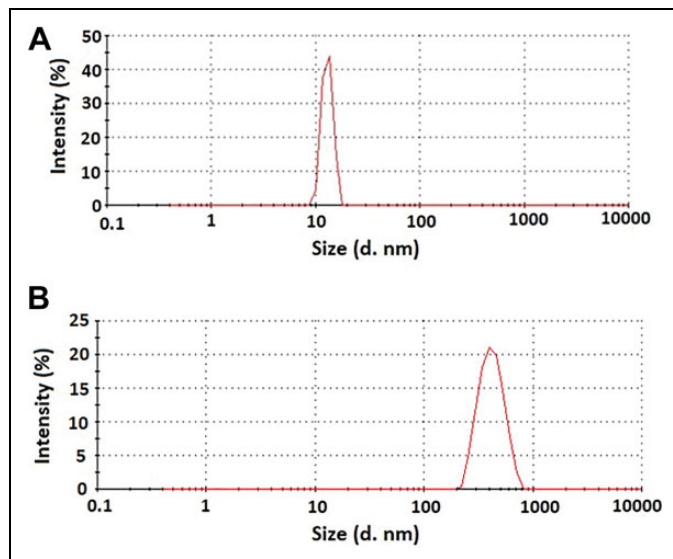


**Figure 1.** Particle size distribution of glimepiride-loaded micelles (A) and nanostructured lipid carriers (B).

**Table 3.** Characteristics of the Prepared Glimepiride Films.

| Run # | Thickness (mm) | Stretching <sup>a</sup> (%) | Drug content (%) |
|-------|----------------|-----------------------------|------------------|
| 1     | 0.54 ± 0.07    | 21.67 ± 2.89                | 129.21 ± 2.20    |
| 2     | 0.50 ± 0.07    | 33.33 ± 2.09                | 119.86 ± 2.44    |
| 3     | 0.41 ± 0.02    | 33.33 ± 4.19                | 128.25 ± 4.16    |
| 4     | 0.62 ± 0.01    | 31.67 ± 3.89                | 101.63 ± 4.21    |
| 5     | 0.32 ± 0.04    | 22.54 ± 1.69                | 102.58 ± 7.71    |
| 6     | 0.39 ± 0.03    | 21.14 ± 4.19                | 129.23 ± 12.23   |
| 7     | 0.71 ± 0.11    | 30.00 ± 1.20                | 105.95 ± 2.66    |
| 8     | 0.49 ± 0.05    | 15.00 ± 5.21                | 98.93 ± 3.04     |
| 9     | 0.43 ± 0.03    | 31.67 ± 5.77                | 118.41 ± 5.35    |
| 10    | 0.79 ± 0.02    | 40.00 ± 8.66                | 116.18 ± 3.7     |
| 11    | 0.66 ± 0.11    | 19.34 ± 2.69                | 108.94 ± 3.63    |
| 12    | 0.45 ± 0.03    | 31.67 ± 2.19                | 129.47 ± 10.20   |
| 13    | 0.57 ± 0.12    | 31.67 ± 4.32                | 108.97 ± 7.59    |
| 14    | 0.31 ± 0.04    | 31.67 ± 3.21                | 110.97 ± 4.03    |
| 15    | 0.68 ± 0.05    | 21.67 ± 3.11                | 105.52 ± 4.01    |

<sup>a</sup>The observed values represent the means of 3 determinations.

introduced in the field of drug delivery to overcome drawbacks arise from older generation lipid-based carriers (as liposomes and solid lipid nanoparticles).<sup>34</sup> The formation of a less ordered lipid matrix with many imperfections of the NLCs system is considered the main advantage of NLCs as it allows for improved solubility and ability to load larger quantities of drugs when compared with other lipid-based carriers.<sup>35-38</sup>

### Characterization of GMD Films

The prepared GMD films were evaluated for the content uniformity, thickness, and stretching. The results obtained for these parameters are summarized in Table 3. Glimepiride content was observed for the examined films of 1 cm<sup>2</sup> containing a theoretical drug concentration of 1 mg of the drug. The results showed

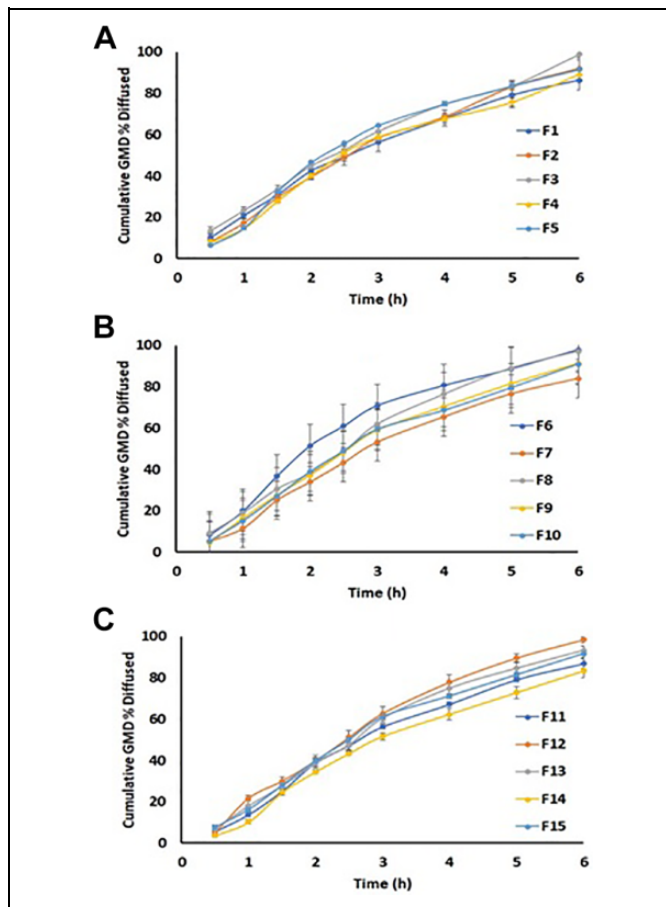


**Figure 2.** Ex vivo permeation profile of glimepiride transmucosal film formulations: F<sub>1</sub> to F<sub>5</sub> (A); F<sub>6</sub> to F<sub>10</sub> (B); and F<sub>11</sub> to F<sub>15</sub> (C).

GMD content of the prepared films ranged from 98.93% ± 3.04% (F<sub>8</sub>) to 129.47% ± 10.20% (F<sub>12</sub>). The film thickness was from 0.31 ± 0.04 mm (F<sub>14</sub>) to 0.79 ± 0.02 mm (F<sub>10</sub>), and the stretching % was ranged from 19.34% ± 2.69% (F<sub>11</sub>) to 40.00% ± 8.66% (F<sub>10</sub>). The GMD-film formulations released most of its GMD content within 6 hours (Figure 2). The values of the initial and cumulative release data for GMD formulations are presented in Table 2. The high GMD content in the prepared films is attributed to the characteristics of the casting method that reduces drug loss during preparation.<sup>20</sup> In addition, film thickness and stretching % are within the acceptable reported limits that indicate the suitability of the method selected and the plasticizer concentration (propylene glycol 2%) used.<sup>39</sup>

### Response Surface Methodology for Optimization of GMD-Loaded Buccal Film

Box-Behnken design was utilized for the optimization of GMD-loaded buccal film with an optimum release profile. The experimental design matrix with different levels of the independent factors is compiled in Table 1. The design of experiment is a multipurpose tool that can help in several aspects. Among these, the optimization technique is simply finding the independent variable values that result in minimizing or maximizing the

objective function subject to constraints, and the desirability functions are used to solve complicated situations that occurred during optimization techniques.<sup>20,39</sup> Response surface methodology has been successfully utilized in several studies to optimize process and formulation variables and to obtain a product with desired properties.<sup>40</sup> Box-Behnken design is one of the efficient response surface methodology tools used mainly to explore and evaluate the main effect, the interaction and the quadratic terms of formulation, and the process variables on the quality attributes of the formulation.<sup>41,42</sup> So, the selection of an experimental design depends on the objectives (or goals) of the experiment as indicated in Table 1.

### Effect of the Independent Variables on the Initial and Cumulative GMD Release ( $Y_1$ and $Y_2$ )

The GMD release is necessary to ensure its availability for absorption in enough concentration to be more effective alongside the use of the film. Release profiles of GMD from the prepared films were represented in Figure 2. The initial and the cumulative GMD release from the films showed marked variations ranged from 10.36% ( $F_{11}$ ) to 23.45% ( $F_6$ ) and 83.27% ( $F_{11}$ ) to 98.71% ( $F_6$ ), respectively (Table 2). The polynomial equations (equations 3 and 4) were generated.

$$\begin{aligned} \text{Initial GMD release } (Y_1) = & 16.714 + 0.085X_1 - 74.7X_2 \\ & + 0.515X_3 - 0.0001X_1^2 \\ & - 0.172X_1X_2 + 0.001X_1X_3 \\ & + 124.67X_2^2 - 2.4X_2X_3 - 0.06X_3^2 \end{aligned} \quad \text{Equation (3)}$$

$$\begin{aligned} \text{Cumulative GMD release } (Y_2) = & 88.9 + 0.103X_1 - 52.6X_2 \\ & + 0.673X_3 + 0.0001X_1^2 \\ & + 0.368X_1X_2 - 0.008X_1X_3 \\ & - 182.67X_2^2 + 8.4X_2X_3 \\ & - 0.079X_3^2 \end{aligned} \quad \text{Equation (4)}$$

Table 4 presents the statistical analysis and Pareto charts presented in Figure 3A showed a significant positive effect of  $X_1$  on the initial release of GMD from the film with a  $P$  value of .0001. This revealed the direct relationship between  $X_1$  and  $Y_1$ , that is, when the percentage of micelles relative to NLCs in the film increased the initial GMD release will increase. On the other hand,  $X_2$  showed a significant negative effect on the initial GMD release from the films with a  $P$  value of .0005. This revealed the inverse relationship between  $X_2$  and  $Y_1$ , that is, when the concentration of CRP in percent increased the initial GMD release will decrease. The effects of the studied factors on the initial GMD release are graphically illustrated in the 3-dimensional response surface plots shown in Figure 3B to D. The same significant effect of these factors was observed on the cumulative GMD release from the prepared films ( $Y_2$ ) with

**Table 4.** Statistical Analysis of Variance of the Responses ( $Y_1$  and  $Y_2$ ) Results.

| Factors        | Initial release ( $Y_1$ ), % |         |                    | Cumulative release ( $Y_2$ ), % |          |                    |
|----------------|------------------------------|---------|--------------------|---------------------------------|----------|--------------------|
|                | Estimate                     | F ratio | P value            | Estimate                        | F ratio  | P value            |
| $X_1$          | 8.8075                       | 444.95  | .0001 <sup>a</sup> | 13.025                          | 11256.26 | .0001 <sup>a</sup> |
| $X_2$          | -3.35                        | 64.37   | .0005 <sup>a</sup> | -2.66                           | 469.46   | .0001 <sup>a</sup> |
| $X_3$          | 1.0175                       | 5.94    | .0589              | 1.47                            | 143.37   | .0001 <sup>a</sup> |
| $X_1X_1$       | 0.7308                       | 1.41    | .2878              | 0.3817                          | 4.46     | .0884              |
| $X_1X_2$       | -0.43                        | 0.53    | .4991              | 0.92                            | 28.08    | .0032 <sup>a</sup> |
| $X_1X_3$       | 0.105                        | 0.03    | .8658              | -0.82                           | 22.31    | .0052 <sup>a</sup> |
| $X_2X_2$       | 0.1558                       | 0.06    | .8099              | -0.2283                         | 1.60     | .2621              |
| $X_2X_3$       | -0.12                        | 0.04    | .8470              | 0.42                            | 5.85     | .0602              |
| $X_3X_3$       | 0.1208                       | 0.04    | .8519              | -0.1583                         | 0.77     | .4210              |
| $R^2$          | 99.043                       |         |                    | 99.958                          |          |                    |
| Adjusted $R^2$ | 97.319                       |         |                    | 99.883                          |          |                    |
| SE             | 0.590                        |         |                    | 0.174                           |          |                    |
| MAE            | 0.287                        |         |                    | 0.075                           |          |                    |

Abbreviations: MAE, mean absolute error; SE, standard error;  $X_1$ , the percentage of micelles relative to NLCs;  $X_2$ , the concentration of CRP in percent;  $X_3$ , the concentration of permeation enhancer in percent;  $X_1X_2$ ,  $X_1X_3$ , and  $X_2X_3$ , the interaction term between the factors;  $X_1X_1$ ,  $X_2X_2$ , and  $X_3X_3$  are the quadratic terms between the factors.

<sup>a</sup>Significant effect of factors on individual responses.

$P$  values of .0001 (Figure 4A). Also, the cumulative GMD release was positively affected significantly with the concentration of permeation enhancer ( $X_3$ ) with a  $P$  value of .0001. Finally, the interaction term between the factors ( $X_1X_2$ ) has an antagonistic significant effect on  $Y_2$  with a  $P$  value of .0032, whereas the interaction term between the factors ( $X_1X_3$ ) has a synergistic significant effect on  $Y_2$  with a  $P$  value of .0052. The effects of the studied factors on the cumulative GMD release are graphically illustrated in the 3-dimensional response surface plots shown in Figure 4B to D.

It is clear from the regression equation 3, the statistical analysis (Table 4), and the Pareto chart (Figure 3A) as well as the response surface plots (Figure 3B-D) that initial % release ( $Y_1$ ) is significantly influenced by  $X_1$  and  $X_2$ , while  $X_3$  had no significant effect on  $Y_1$ . An increase in the percentage of micelles relative to NLCs in the film ( $X_1$ ) from 0% to 100%, at the same level of  $X_2$  and  $X_3$ , led to an increase in  $Y_1$  from 13.96% to 23.45% for  $F_2$  and  $F_6$ , respectively. Also, it is obvious from the regression equation 4, the statistical analysis (Table 4) and the Pareto chart (Figure 4A) as well as the response surface plots (Figure 4B-D) that the cumulative % release ( $Y_2$ ) is significantly influenced by  $X_1$ ,  $X_2$ , and  $X_3$ . An increase in the percentage of micelles relative to NLCs in the film ( $X_1$ ) from 0% to 100%, at the same level of  $X_2$  and  $X_3$ , led to an increase in  $Y_2$  from 86.83% to 98.93% for  $F_2$  and  $F_6$ , respectively. A similar trend was observed with a direct relationship between  $Y_2$  and the concentration of permeation enhancer in percent ( $X_3$ ).

The enhancement in the initial and the cumulative % release could be attributed to increase the solubility of GMD in TPGS micellar vesicles. The improved solubility of GMD and other drugs by TPGS micelles is the result of the elevated hydrophilic-lipophilic balance value of TPGS (13.2).<sup>15,30</sup> The amphiphilic

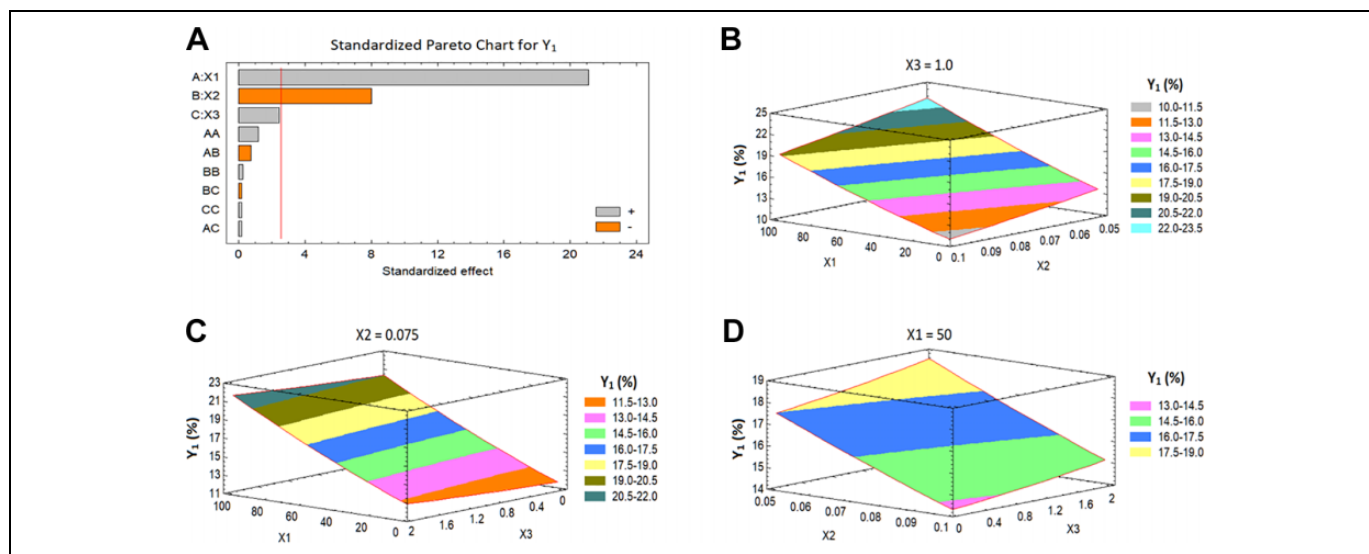


**Figure 3.** Pareto chart (A) and Response surface plots (B-D) for  $Y_1$ .

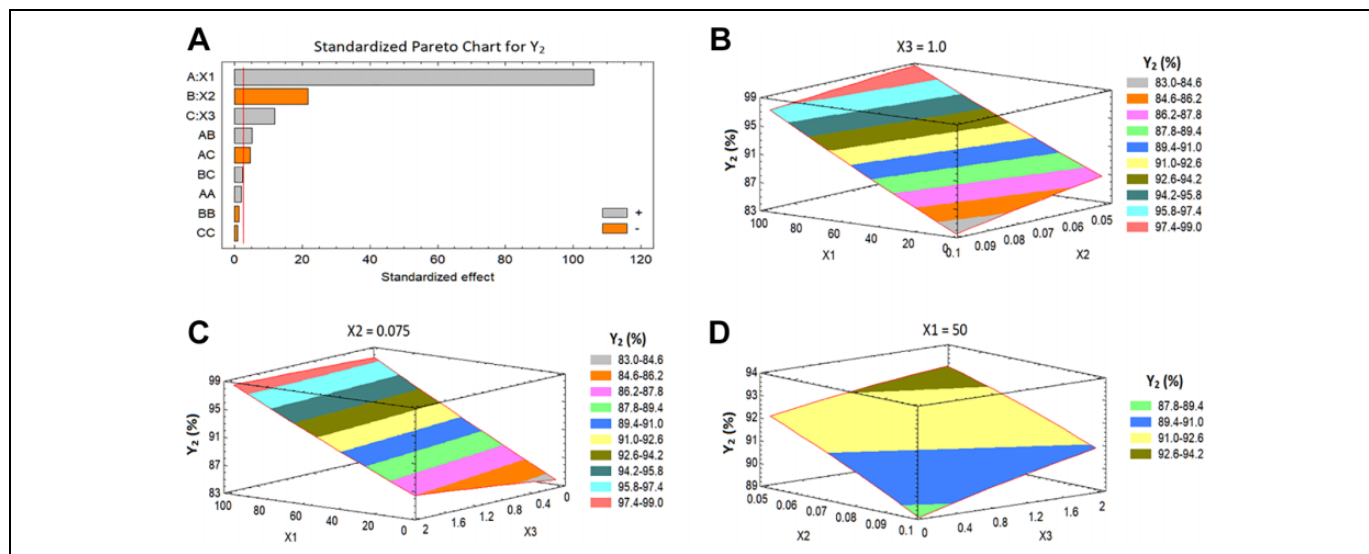


**Figure 4.** Pareto chart (A) and Response surface plots (B-D) for  $Y_2$ .

TPGS structure that includes vitamin E, the hydrophobic portion, and PEG, the hydrophilic one has the ability to inhibit P-glycoprotein responsible for drug efflux from the cells that enhances the cellular uptake of GMD.<sup>15,40,41</sup> In addition, the reported antioxidant characters of TPGS could protect incorporated drugs from oxidative degradation during storage. Also, the reported TPGS critical micelle concentration is 0.02% (wt/wt) and the concentration used in this investigation was above this concentration to ensure thermodynamically stable micelles formation. The direct relationship between  $Y_2$  and the concentration of permeation enhancer ( $X_3$ ) could be related to the reversible destabilizing the membrane lipid bilayer that leads to increased membrane fluidity and enhanced drug permeability.<sup>42-44</sup>

An opposite trend was observed with an inverse relationship between both  $Y_1$  and  $Y_2$  and the concentration of CRP in the film

matrix ( $X_2$ ). An increase in the concentration of  $X_2$  from 0.05% to 1%, at the same level of  $X_1$  and  $X_3$ , led to a decrease in  $Y_1$  and  $Y_2$  from 13.96% to 10.36% and from 86.91% to 83.27% for  $F_2$  and  $F_{11}$ , respectively. Also, the same finding was confirmed for  $F_{12}$  and  $F_8$  that illustrated a decrease in the  $Y_1$  value from 18.02% to 15.23%, and  $Y_2$  from 93.15% to 90.97%, respectively. This could be attributed to that CRP is a cross-linked polymer that shows increased viscosity with increased concentration and the reduced cumulative % release could be related to the viscosity of diffusion layer that hinders drug permeation from the more viscous matrix.<sup>45</sup> The highly viscous layer formed as a result of the hydrated polymer chain act as a resistance layer for GMD diffusion.<sup>20</sup> Accordingly, CRP showed a significant inverse relationship with  $Y_2$ . Carbopol showed the same trend with  $Y_1$  although nonsignificant, this could be related to the increased

**Table 5.** Composition of the Optimized Glimepiride-Loaded Buccal Film With the Observed, Fitted, and Residual Values.

| Factor   | Optimum | Response                                | Observed value | Fitted value | Residual |
|--|---------|---|----------------|--------------|----------|
| X <sub>1</sub> : The percentage of micelles relative to NLCs | 99.92   | Y <sub>1</sub> : Initial release (%)    | 21.43          | 23.4955      | 2.07     |
| X <sub>2</sub> : The percentage of CRP                       | 0.05    | Y <sub>2</sub> : Cumulative release (%) | 95.10          | 98.9604      | 3.86     |
| X <sub>3</sub> : The percentage of permeation enhancer       | 1.8     |   |                |              |          |

Abbreviations: CRP, Carbopol; NLCs, nanostructured lipid carriers.

concentration of GMD in the superficial layers of the film during drying that could induce a burst effect at the start of the diffusion study. Accordingly, CRP showed a significant inverse relation with Y<sub>2</sub>, but not significant with Y<sub>1</sub>.

### Prediction of the Optimized GMD-Loaded Buccal Film

Numerical optimization following the desirability function approach was applied to predict the optimum GMD-loaded buccal film composition with an optimum GMD-release profile. The optimum level of the independent factor was found to be 99.92% of the micelles relative to NLCs, 0.05 the percentage of CRP, and 1.8% of the permeation enhancer. This combination of factor levels maximized the desirability function over the indicated region to be 1.0. Also, the optimized GMD-loaded buccal films exhibited an acceptable release profile. The observed parameters were in good agreement with the predicted ones with a percentage error of less than 5% as indicated in Table 5. The predicted values for Y<sub>1</sub> and Y<sub>2</sub> were 23.496% and 98.96%, respectively, and the residual values for both responses were 2.07% and 3.86%, respectively.

### Mucoadhesive Test for the Optimized GMD Film

The optimized GMD film showed a tensile strength of 0.01390 N/mm<sup>2</sup>. Tensile strength provides a quantitative tool for the degree of GMD film binding to the buccal epithelia.<sup>25</sup> The high viscosity grade of HPMC (film-forming polymer) is attributed to increased mucoadhesive strength and residence time.<sup>46</sup> Swelling characters and the formation of strong hydrogen bonding with mucin are attributed to the mucoadhesion behavior of HPMC.<sup>47,48</sup> In addition, CRP is reported for its mucoadhesive character that augments the mucoadhesive properties of HPMC film. The repulsion forces between ionized carboxylate moiety, on CRP backbone (pK around 6.0), at pH of the buccal cavity (6.2-7.6) that leads to swelling of CRP.<sup>49,50</sup> The hydration ability of CRP enhances its mucoadhesive characters and facilitates long residence and prolonged release of GMD. Water molecules bind to the polymer carboxyl groups, which are required for adhesion and swelling.<sup>51</sup>

### Preparation of Unidirectional-Release GMD Films

Bilayer oromucosal film preparations (buccal films) offer a promising way to enable drug administration via the oral cavity. Adding a nonsoluble or slowly eroding/dissolving backing layer to a mucoadhesive drug-loaded layer enables unidirectional drug delivery.<sup>52</sup> In the present study, a bilayer buccal

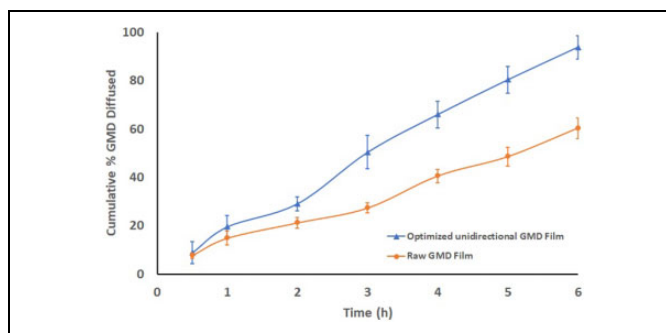


**Figure 5.** Ex vivo permeation profile of optimized glimepiride transmucosal film formulation.

film was developed by coating the prepared optimized buccal polymeric matrix film from one side using 2% ethylcellulose. This coating aimed to achieve unidirectional release toward the oral mucosa (bilayered film) that avoids drug release in the oral cavity and provides taste masking of the film to increase patient compliance, which in accordance with the previously reported studies.<sup>28,53</sup> Bilayer devices should release the drug in a unidirectional way toward the mucosa (to avoid loss of drug due to washing out by saliva), in a controlled and predictable manner, to elicit the required therapeutic response.<sup>52</sup>

### Ex Vivo Release Profile of GMD From the Optimized Bilayer Film

The ex vivo release profile of GMD from the optimized unidirectional GMD transmucosal film in comparison with the film containing raw GMD is shown in Figure 5. The optimized buccal film showed improved GMD-release behavior when compared with the film containing raw GMD. The optimized unidirectional GMD transmucosal film showed a release of 93.9% of GMD content at 6 hours compared to 60.41% of GMD release from the raw GMD film.

The higher HPMC content in films causes more swelling ratio, which increases film thickness. Therefore, the HPMC layer can reduce drug diffusion, which was confirmed by other groups working with HPMC-based buccal films.<sup>46,54,55</sup> The side of the optimized film directed toward the buccal cavity was coated with ethylcellulose, aiming to prevent GMD release to the buccal cavity and ingestion to the gastrointestinal tract. Ethylcellulose is a water-insoluble polymer that is utilized in the formulation of controlled-release behavior. Ethylcellulose is a film-forming and nonionic material that has the advantage of being nonreactive.<sup>56</sup>

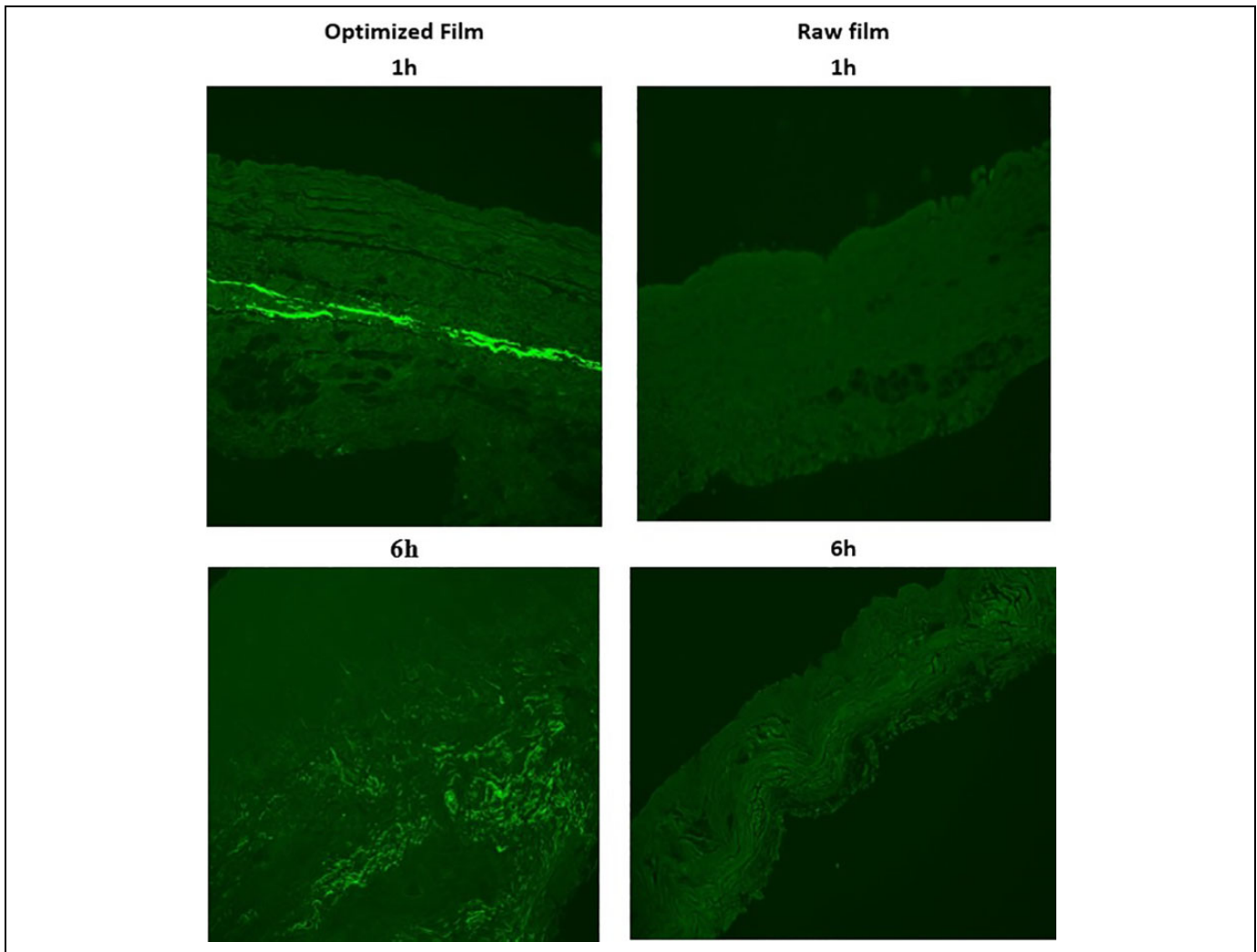


**Figure 6.** Fluorescence laser microscope image in cheap mucosa following transdermal application of fluorescence isothiocyanate (control) after 1 and 6 hours.

### Fluorescence Laser Microscope Study

The transport of pure FITC-containing film (control) and fluorescence-labeled optimized formulation of transmucosal film is illustrated in Figure 6. Unlike the pure FITC, the optimized formulation was able to transport across the buccal mucosa, which was confirmed by the intensity of fluorescence. The diffusion of the pure FITC was restricted to the outer buccal layer. These results indicate the successful delivery of the optimized formulation to deeper buccal layers. Our result is in good agreement with previous reports indicating the effectiveness of nanocarrier systems in skin permeation and delivery.<sup>57,58</sup> Accordingly, the optimized formulation showed a promise for improved absorption and bioavailability of GMD loaded into the nanocarrier-loaded film formula.

### Conclusions

The formulation variables of the transmucosal buccal film were optimized using BBD. The mathematical design succeeded to

optimize the factors that enhance the release of GMD from a unidirectional transmucosal film loaded with TPGS micelles in a controlled and predictable manner. The optimized formulation revealed that the permeation of GMD from the film was in favor of TPGS micelles. The optimized unidirectional GMD transmucosal film showed a release of 93.9% of GMD content at 6 hours compared to 60.41% of GMD release from the raw GMD film. This result was confirmed by its ability to transport across the buccal mucosa, which revealed by the intensity of fluorescence with the fluorescence-labeled optimized formulation. This finding confirmed the suitability of transmucosal delivery of GMD via the buccal mucosa in a sustained-release pattern.

### Acknowledgments

The authors, therefore, acknowledge with thanks DSR for technical and financial support.

### Declaration of Conflicting Interests

The author(s) declared no potential conflicts of interest with respect to the research, authorship, and/or publication of this article.

## Funding

The author(s) disclosed receipt of the following financial support for the research, authorship, and/or publication of this article: This project was funded by the Deanship of Scientific Research (DSR) at King Abdulaziz University, Jeddah, under grant no. (RG-6-166-40).

## ORCID iD

Osama A. A. Ahmed  <https://orcid.org/0000-0002-3204-381X>

## References

- American Diabetes Association. Diagnosis and classification of diabetes mellitus. *Diabetes Care*. 2014;37(suppl 1):S81-S90. doi: 10.2337/dc14-S081
- Weitgasser R, Lechleitner M, Luger A, Klingler A. Effects of glimepiride on HbA1c and body weight in type 2 diabetes: results of a 1.5-year follow-up study. *Diabetes Res Clin Pract*. 2003; 61(1):13-19. doi:10.1016/S0168-8227(02)00254-1
- Massi-Benedetti M. Glimepiride in type 2 diabetes mellitus: a review of the worldwide therapeutic experience. *Clin Ther*. 2003;25(3):799-816. doi:10.1016/S0149-2918(03)80109-1
- Kiran T, Shastri N, Ramakrishna S, Sadanandam M. Surface solid dispersion of glimepiride for enhancement of dissolution rate. *Int J PharmTech Res*. 2009;1(3):822-831.
- Frick A, Möller H, Wirbitzki E. Biopharmaceutical characterization of oral immediate release drug products. In vitro/in vivo comparison of phenoxymethylpenicillin potassium, glimepiride and levofloxacin. *Eur J Pharm Biopharm*. 1998;46(3):305-311. doi:10.1016/S0939-6411(98)00041-1
- Davis SN. The role of glimepiride in the effective management of type 2 diabetes. *J Diabetes Complicat*. 2004;18(6):367-376. doi: 10.1016/j.jdiacomp.2004.07.001
- Vidyadhara S, Babu JR, Sasidhar RLC, et al. Pharmed formulation and evaluation of glimepiride solid dispersions and their tablet formulations for enhanced bioavailability. *Pharmed*. 2011;2(February):15-20.
- Banga AK, Chien YW. Systemic delivery of therapeutic peptides and proteins. *Int J Pharm*. 1988;48(1-3):15-50. doi:10.1016/0378-5173(88)90246-3
- Salamat-Miller N, Chittchang M, Johnston TP. The use of mucoadhesive polymers in buccal drug delivery. *Adv Drug Deliv Rev*. 2005;57(11):1666-1691. doi:10.1016/j.addr.2005.07.003
- Ananda Reddy K, Venugopal K. Formulation and in vitro evaluation of buccal tablets of piroxicam. *Int J Chem Sci*. 2012;10(1): 399-412.
- Woodley J. Bioadhesion: new possibilities for drug administration? *Clin Pharmacokinet*. 2001;40(2):77-84. doi:10.2165/00003088-200140020-00001
- Yadav N, Khatak S, Singh Sara UV. Solid lipid nanoparticles – a review. *Int J Appl Pharm*. 2013;5(2):8-18. doi:10.9790/3013-26103444
- Lason E, Sikora E, Ogonowski J. Influence of process parameters on properties of nanostructured lipid carriers (NLC) formulation. *Acta Biochim Pol*. 2013;60(4):773-777. doi:10.18388/abp.2013\_2056
- Kaneda Y. Virosomes: evolution of the liposome as a targeted drug delivery system. *Adv Drug Deliv Rev*. 2000;43(2-3): 197-205. doi:10.1016/S0169-409X(00)00069-7
- Yang C, Wu T, Qi Y, Zhang Z. Recent advances in the application of vitamin E TPGS for drug delivery. *Theranostics*. 2018;8(2): 464-485. doi:10.7150/thno.22711
- Somagoni J, Boakye CHA, Godugu C, et al. Nanomielgel – a novel drug delivery system for topical application – in vitro and in vivo evaluation. Jablonski MM, ed. *PLoS One*. 2014;9(12): e115952. doi:10.1371/journal.pone.0115952
- Liu Z, Zhang X, Wu H, et al. Preparation and evaluation of solid lipid nanoparticles of baicalin for ocular drug delivery system in vitro and in vivo. *Drug Dev Ind Pharm*. 2011;37(4):475-481. doi: 10.3109/03639045.2010.522193
- El-Helw AR, Fahmy UA. Improvement of fluvastatin bioavailability by loading on nanostructured lipid carriers. *Int J Nanomed*. 2015;10:5797-5804. doi:10.2147/IJN.S91556
- Nesseem DI, Eid SF, El-Houseny SS. Development of novel transdermal self-adhesive films for tenoxicam, an anti-inflammatory drug. *Life Sci*. 2011;89(13-14):430-438. doi:10.1016/j.lfs.2011.06.026
- Ahmed OAA, Kurakula M, Banjar ZM, Afouna MI, Zidan AS. Quality by design coupled with near infrared in formulation of transdermal glimepiride liposomal films. *J Pharm Sci*. 2015; 104(6):2062-2075. doi:10.1002/jps.24448
- Gupta S, Samanta MK, Raichur AM. Dual-drug delivery system based on in situ gel-forming nanosuspension of forskolin to enhance antiglaucoma efficacy. *AAPS PharmSciTech*. 2010; 11(1):322-335. doi:10.1208/s12249-010-9388-x
- Ahmed TA. Formulation and clinical investigation of optimized vinpocetine lyopant-tabs: new strategy in development of buccal solid dosage form. *Drug Des Devel Ther*. 2019;13:205-220. doi: 10.2147/DDDT.S189105
- El-Enany NM, Abdelal AA, Belal FF, Itoh YI, Nakamura MN. Development and validation of a rephased phase – HPLC method for simultaneous determination of rosiglitazone and glimepiride in combined dosage forms and human plasma. *Chem Cent J*. 2012;6(1):9. doi:10.1186/1752-153X-6-9
- Ahmed OAOAA, Afouna MIMI, El-Say KMKM, et al. Optimization of self-nanoemulsifying systems for the enhancement of in vivo hypoglycemic efficacy of glimepiride transdermal patches. *Expert Opin Drug Deliv*. 2014;11(7):1005-1013. doi:10.1517/17425247.2014.906402
- Nair AB, Kumria R, Harsha S, et al. In vitro techniques to evaluate buccal films. *J Control Release*. 2013;166(1):10-21. doi:10.1016/j.jconrel.2012.11.019
- Darwesh B, Aldawsari HM, Badr-Eldin SM. Optimized chitosan/anion polyelectrolyte complex based inserts for vaginal delivery of fluconazole: in vitro/in vivo evaluation. *Pharmaceutics*. 2018; 10(4):227. doi:10.3390/pharmaceutics10040227
- Wang L, Tang X. A novel ketoconazole bioadhesive effervescent tablet for vaginal delivery: design, in vitro and “in vivo” evaluation. *Int J Pharm*. 2008;350(1-2):181-187. doi:10.1016/j.ijpharm.2007.08.042
- Abruzzo A, Nicoletta FP, Dalena F, et al. Bilayered buccal films as child-appropriate dosage form for systemic administration of

- propranolol. *Int J Pharm.* 2017;531(1):257-265. doi:10.1016/j.ijpharm.2017.08.070
29. Patra JK, Das G, Fraceto LF, et al. Nano based drug delivery systems: recent developments and future prospects. *J Nanobiotechnol.* 2018;16(1):1-33. doi:10.1186/s12951-018-0392-8
30. Guo Y, Luo J, Tan S, Otieno BO, Zhang Z. The applications of vitamin E TPGS in drug delivery. *Eur J Pharm Sci.* 2013;49(2):175-186. doi:10.1016/J.EJPS.2013.02.006
31. Ahmed OAA, Badr-Eldin SM. In situ misemgel as a multifunctional dual-absorption platform for nasal delivery of raloxifene hydrochloride: formulation, characterization, and in vivo performance. *Int J Nanomed.* 2018;13:6325-6335. doi:10.2147/IJN.S181587
32. Gaba B, Fazil M, Ali A, et al. Nanostructured lipid (NLCs) carriers as a bioavailability enhancement tool for oral administration. *Drug Deliv.* 2015;22(6):691-700. doi:10.3109/10717544.2014.898110
33. Montenegro L, Lai F, Offerta A, et al. From nanoemulsions to nanostructured lipid carriers: a relevant development in dermal delivery of drugs and cosmetics. *J Drug Deliv Sci Technol.* 2016;32:100-112. doi:10.1016/J.JDDST.2015.10.003
34. Dingler A, Blum RP, Niehus H, Müller RH, Gohla S. Solid lipid nanoparticles (SLN(TM)/Lipopearls(TM)) – a pharmaceutical and cosmetic carrier for the application of vitamin E in dermal products. *J Microencapsul.* 1999;16(6):751-767. doi:10.1080/026520499288690
35. Muller RH, Keck CM. Challenges and solutions for the delivery of biotech drugs – a review of drug nanocrystal technology and lipid nanoparticles. *J Biotechnol.* 2004;113(1-3):151-170. doi:10.1016/j.jbiotec.2004.06.007
36. Khosa A, Reddi S, Saha RN. Nanostructured lipid carriers for site-specific drug delivery. *Biomed Pharmacother.* 2018;103:598-613. doi:10.1016/j.biopha.2018.04.055
37. Tiwari R, Pathak K. Nanostructured lipid carrier versus solid lipid nanoparticles of simvastatin: comparative analysis of characteristics, pharmacokinetics and tissue uptake. *Int J Pharm.* 2011;415(1-2):232-243. doi:10.1016/j.ijpharm.2011.05.044
38. Beloqui A, del Pozo-Rodríguez A, Isla A, et al. Nanostructured lipid carriers as oral delivery systems for poorly soluble drugs. *J Drug Deliv Sci Technol.* 2017;42:144-154. doi:10.1016/j.jddst.2017.06.013
39. El-Maghraby GM, Abdelzaher MM. Formulation and evaluation of simvastatin buccal film. *J Appl Pharm Sci.* 2015;5(4):70-77. doi:10.7324/JAPS.2015.50412
40. Zhang Z, Tan S, Feng SSSS. Vitamin E TPGS as a molecular biomaterial for drug delivery. *Biomaterials.* 2012;33(19):4889-4906. doi:10.1016/j.biomaterials.2012.03.046
41. Dintaman JM, Silverman JA. Inhibition of P-glycoprotein by D-alpha-tocopheryl polyethylene glycol 1000 succinate (TPGS). *Pharm Res.* 1999;16(10):1550-1556. Accessed February 19, 2019. <http://www.ncbi.nlm.nih.gov/pubmed/10554096>
42. Bejugam NK, Parish HJ, Shankar GN. Influence of formulation factors on tablet formulations with liquid permeation enhancer using factorial design. *AAPS PharmSciTech.* 2009;10(4):1437-1443. doi:10.1208/s12249-009-9345-8
43. Taghizadeh SM, Moghimi-Ardakani A, Mohamadnia F. A statistical experimental design approach to evaluate the influence of various penetration enhancers on transdermal drug delivery of buprenorphine. *J Adv Res.* 2015;6(2):155-162. doi:10.1016/j.jare.2014.01.006
44. Magnusson BM, Runn P. Effect of penetration enhancers on the permeation of the thyrotropin releasing hormone analogue pGlu-3-methyl-His-Pro amide through human epidermis. *Int J Pharm.* 1999;178(2):149-159. doi:10.1016/S0378-5173(98)00316-0
45. Jones DS, Woolfson AD, Brown AF. Textural, viscoelastic and mucoadhesive properties of pharmaceutical gels composed of cellulose polymers. *Int J Pharm.* 1997;151(2):223-233. doi:10.1016/S0378-5173(97)04904-1
46. Shanker G, Kumar CK, Gonugunta CSR, Kumar BV, Veerareddy PR. Formulation and evaluation of bioadhesive buccal drug delivery of tizanidine hydrochloride tablets. *AAPS PharmSciTech.* 2009;10(2):530-539. doi:10.1208/s12249-009-9241-2
47. Kim TH, Ahn JS, Choi HK, Choi YJ, Cho CS. A novel mucoadhesive polymer film composed of carbopol, poloxamer and hydroxypropylmethylcellulose. *Arch Pharm Res.* 2007;30(3):381-386. doi:10.1007/bf02977622
48. El Sharawy AM, Shukr MH, Elshafeey AH. Formulation and optimization of duloxetine hydrochloride buccal films: In vitro and in vivo evaluation. *Drug Deliv.* 2017;24(1):1762-1769. doi:10.1080/10717544.2017.1402216
49. Bera K, Mazumder B, Khanam J. Study of the mucoadhesive potential of carbopol polymer in the preparation of microbeads containing the antidiabetic drug glipizide. *AAPS PharmSciTech.* 2016;17(3):743-756. doi:10.1208/s12249-015-0396-8
50. Patel JK, Chavda JR. Formulation and evaluation of stomach-specific amoxicillin-loaded carbopol-934P mucoadhesive microspheres for anti-*Helicobacter pylori* therapy. *J Microencapsul.* 2009;26(4):365-376. doi:10.1080/02652040802373012
51. Deasy PB, Collins AEM, Maccarthy DJ, Russell RJ. Use of strips containing tetracycline hydrochloride or metronidazole for the treatment of advanced periodontal disease. *J Pharm Pharmacol.* 1989;41(10):694-699. doi:10.1111/j.2042-7158.1989.tb06343.x
52. Patel VM, Prajapati BG, Patel HV, Patel KM. Mucoadhesive bilayer tablets of propranolol hydrochloride. *AAPS PharmSciTech.* 2007;8(3):E203-E208. doi:10.1208/pt0803077
53. Swamy PV, Kinagi MB, Biradar SS, Gada SN, Shilpa H. Formulation design and evaluation of bilayer buccal tablets of granisetron hydrochloride. *Indian J Pharm Educ Res.* 2011;45(3):242-247.
54. Salehi S, Boddohi S. New formulation and approach for mucoadhesive buccal film of rizatriptan benzoate. *Prog Biomater.* 2017;6(4):175-187. doi:10.1007/s40204-017-0077-7
55. Kumria R, Nair AB, Goomber G, Gupta S. Buccal films of prednisolone with enhanced bioavailability. *Drug Deliv.* 2016;23(2):471-478. doi:10.3109/10717544.2014.920058
56. Wasilewska K, Winnicka K. Ethylcellulose – a pharmaceutical excipient with multidirectional application in drug dosage forms development. *Materials (Basel).* 2019;12(20):3386. doi:10.3390/ma12203386

57. Ahmed OAAA, El-Say KM, Aljaeid BM, Badr-Eldin SM, Ahmed TA. Optimized vinpocetine-loaded vitamin E D- $\alpha$ -tocopherol poly-ethylene glycol 1000 succinate-alpha lipoic acid micelles as a potential transdermal drug delivery system: in vitro and ex vivo studies. *Int J Nanomedicine*. 2018;14:33-43. doi:10.2147/IJN.S187470
58. Ahmed TA, Alay AMS, Okbazghi SZ, Alhakamy NA. Two-step optimization to develop a transdermal film loaded with dapoxetine nanoparticles: a promising technique to improve drug skin permeation. *Dose-Response*. 2020;18(2):155932582092385. doi:10.1177/1559325820923859